Environ Monit Assess (2014) 186:1203–1217
DOI 10.1007/s10661-013-3450-6

Artificial neural network modeling of dissolved oxygen in reservoir

Wei-Bo Chen · Wen-Cheng Liu

Received: 25 May 2013 / Accepted: 14 September 2013 / Published online: 28 September 2013

Abstract The water quality of reservoirs is one of the key factors in the operation and water quality management of reservoirs. Dissolved oxygen (DO) in water column is essential for microorganisms and a significant indicator of the state of aquatic ecosystems. In this study, two artificial neural network (ANN) models including back propagation neural network (BPNN) and adaptive neural-based fuzzy inference system (ANFIS) approaches and multilinear regression (MLR) model were developed to estimate the DO concentration in the Feitsui Reservoir of northern Taiwan. The input variables of the neural network are determined as water temperature, pH, conductivity, turbidity, suspended solids, total hardness, total alkalinity, and ammonium nitrogen. The performance of the ANN models and MLR model was assessed through the mean absolute error, root mean square error, and correlation coefficient computed from the measured and model-simulated DO values. The results reveal that ANN estimation performances were superior to those of MLR. Comparing to the BPNN and ANFIS models through the performance criteria, the ANFIS model is better than the BPNN model for predicting the DO values. Study results show that the neural network particularly using ANFIS model is able to predict the DO concentrations with reasonable accuracy, suggesting that the neural network is a valuable tool for reservoir management in Taiwan.

Keywords Dissolved oxygen · Reservoir · Artificial neural network · Multilinear regression · Water quality modeling

W.-B. Chen
National Science and Technology Center for Disaster Reduction, New Taipei City 23143, Taiwan

W.-C. Liu (✉)
Department of Civil and Disaster Prevention Engineering, National United University, Miaoli 36003, Taiwan
e-mail: wcliu@nuu.edu.tw

W.-C. Liu
Taiwan Typhoon and Flood Research Institute, National Applied Research Institute, Taipei 10093, Taiwan

Introduction

Modeling water quality variables is a very important aspect of the analysis of any aquatic system. The chemical, physical, and biological components of aquatic ecosystems are very complex and nonlinear. Numerous computational and statistical approaches have been applied to predict the water quality in reservoirs (Liu et al. 2009; Cho et al. 2009; White et al. 2010; Lindim et al. 2011).

Dissolved oxygen (DO) is one of the important water quality parameters for aquatic life and for other uses of water. Sufficient DO is essential for good water quality since oxygen is needed in a water body to support aquatic life and basic oxygen demand (decomposition of organic matter). Quantification of DO in reservoirs is one of the primary concerns of limnologists and water resources engineers. Applications of different approaches to quantify DO levels in reservoirs have been documented. There are two approaches including deterministic and statistical/stochastic models used to predict the DO in a water column. Dynamic (deterministic) models with hydrodynamic transport modeling components involve the solution of differential equations, which formulate the relevant physical, chemical, and biological mechanisms

and interactions as ecological formulations (Bonnet and Poulin 2004; Stansbury et al. 2008; Rucinski et al. 2010; Karakaya et al. 2011). The process-based modeling approaches can provide good estimations of water quality variables, but they usually are too general to be applied directly without a lengthy data calibration process. They often require approximations of various processes, and these approximations may overlook some important factors affecting the processes in reservoirs.

The other approach is statistical/stochastic model which uses the water quality data to establish the predictive model (Curi et al. 1995; Boano et al. 2006). Many statistically based water quality models assume a linear relationship between response and prediction variables and their normal distribution. However, the DO dynamics is highly nonlinear and many useful statistical theories cannot be implemented and used for predicting DO.

Although parametric statistical and deterministic models have been adopted for modeling water quality, they require a lot of input data, model parameters, and vast information on various hydrological subprocesses in order to achieve the end results. Since a large number of factors affecting the water quality have a complicated nonlinear relationship with the variables, traditional data processing methods are no longer applicable for solving the problem. In recent years, several researches have been conducted on water quality simulation using artificial neural network (ANN) models (Palani et al. 2008; Singh et al. 2009; Soltani et al. 2010; Yao et al. 2011; Najah et al. 2011, 2012; Rankovic et al. 2012; Wen et al. 2013). The ANN approach has several advantages over traditional phenomenological or semiempirical models, because it requires known input data set without any assumptions. The ANN develops a mapping of the input and output variables which can subsequently be used to predict the desired output as a function of suitable inputs. A multilayer neural network can approximate any smooth, measurable function between input and output vectors by selecting a suitable set of connecting weights and transfer functions (Gardner and Dorling 1998). Disadvantages of the ANN approach include its black box nature, proneness to overfitting, and the empirical nature of model development.

The adaptive neural-based fuzzy inference system (ANFIS) model and its principles proposed by Jang (1992) have been applied to study many problems. The model identifies a set of parameters through a hybrid learning rule combining the back propagation gradient descent and a least squares method. It can be used as a basis for constructing a set of fuzzy IF–THEN rules with appropriate membership functions in order to generate the previously stipulated input–output pairs. ANFIS has faster convergence than a typical feed-forward network. Its model is compact and thus requires smaller size training set. It also provides automatic tuning of parameters in fuzzy logic control. In ANFIS, the smoothness is provided by interpolation in fuzzy control and the adaptability by neural networks. For trade-off between neural and fuzzy systems, ANFIS is the best approach. But with these advantages, ANFIS has some drawbacks such as it can cause surface oscillations around points due to high partition number, spatial complexity increases exponentially, and awkward interpolation occurs between slopes of different signs if fuzzy logic control interface mechanism is used for interpolation among rules.

The ANFIS model has been widely successfully applied for various water resources and water quality problems. For example, Keskin et al. (2006) applied the ANFIS model to river flow prediction in Dim Stream in the southern part of Turkey. Soltani et al. (2010) developed a new methodology combining water quality simulation model and a hybrid genetic algorithm for determining optimal operating policies for different reservoir outlets. The water quality simulation model was based on some ANFIS models, which were trained and tested using the results of a calibrated water quality simulated model. Talei et al. (2010) investigated the effects of the input used on event-based runoff forecasting by ANFIS. Fifteen ANFIS models were compared, differentiated by the choice of rainfall and/or discharge inputs used. Nourani and Komasi (2013) developed an integrated geomorphological adaptive neuro-fuzzy inference system (IGANFIS) model conjugated with C-means clustering algorithm for rainfall-runoff modeling at multiple stations of the Eel River Watershed. Rezaeianzadeh et al. (2013) presented the use of ANN, ANFIS, multiple linear regression, and multiple nonlinear regression for forecasting maximum daily flow at the outlet of the Khosrow Shirin Watershed, located in the Fars Province of Iran.

The main aim of the present work is to construct a multilinear regression model (MLR) and two ANN models including back propagation neural network and ANFIS to predict the DO in the Feitsui Reservoir of northern Taiwan and demonstrate its application to identifying complex nonlinear relationships between input and output. The comparisons of predicted and

measured DO values were implemented using the multilinear regression and two ANN models.

Material and methods

Description of study area

The Feitsui Reservoir, serving as the source of domestic water supply for the Taipei Metropolitan Area with a population of over five million, was completed on 1987 with an initial storage of 406×10^6 m^3. The main dam is located at the downstream of Peishih Creek, a tributary of Hsintien Creek (Fig. 1). The reservoir has a surface area (at EL. 170 m) of 10.24 km^2 and a mean depth of 40 m with a maximum depth of 113.4 m near the dam. The average water residence time in the reservoir is approximately 150 days. The reservoir is one of the most monitored reservoirs in Taiwan.

The Feitsui Reservoir is located in an area with a subtropical oceanic climate, and its annual mean air temperature is between 18 and 23 °C. Typhoons bring huge amount of water in summer and autumn, whereas monsoons bring cold fronts with abundant precipitation in winter. The mean annual precipitation and inflow into the reservoir were 3,784 and 3,214 mm from 1989 to 2007. The highest and lowest water temperatures in the reservoir were 33.5 and 14.4 °C, in August and February, respectively. The average was 22.0±4.8 °C. The water temperature in hypolimnion was nearly constant at 16.0±0.3 °C. The reservoir thus has a monomictic type of thermal circulation (Chen and Wu 2006).

A survey showed that the major types of land use in the Feitsui Watershed were forestland (about 88 % of the

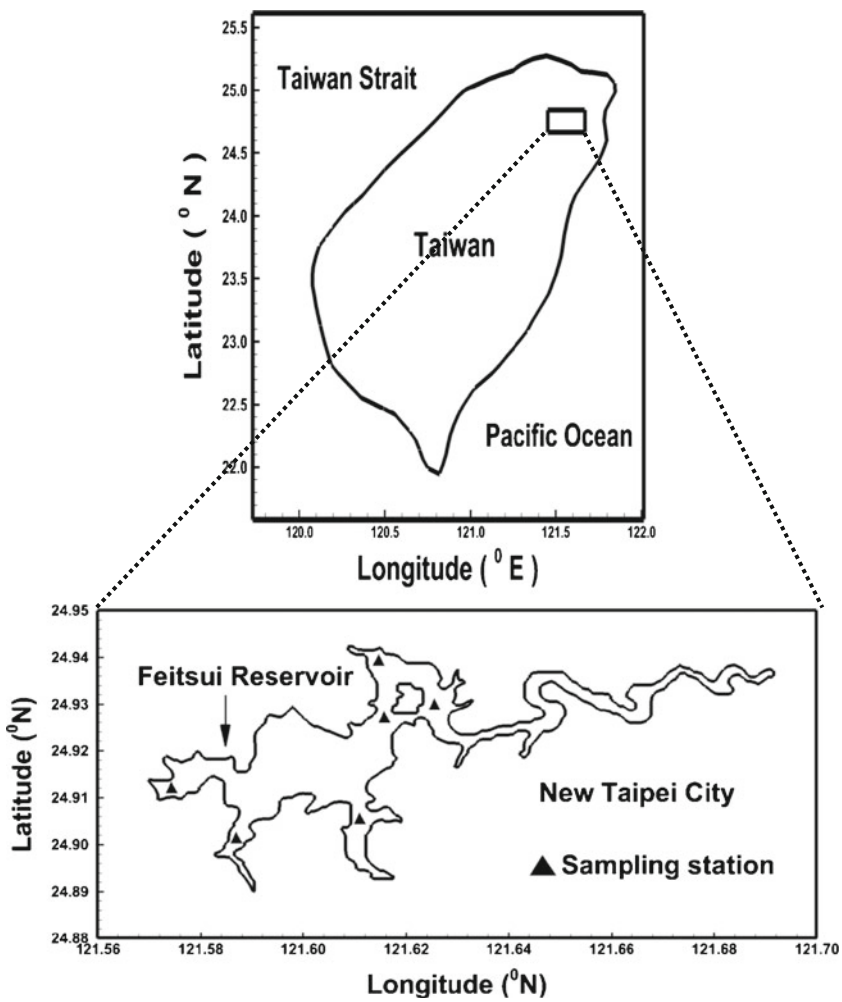

Fig. 1 Map of the study area and water quality sampling stations

total area of watersheds) and tea garden (about 4 % of the total area of watersheds), both of which contribute to pollution of nonpoint sources (Chou et al. 2007). Based on *A report of implementation efficiency on protecting water quality/quantity for Taipei Water Source Domain*, published by the Taipei Water Management Committee (TWMC 2003), the sources of point source pollution included domestic wastewater (lack of sewers area) and wastewater produced by leisure activities. The loading of total phosphorus (TP) was estimated on the basis of population and its equivalent. The population was surveyed which included 8,576 residents and 392,400 visitors per year. And 8 mg TP/L of the equivalent concentration of wastewater was employed. The discharge of each resident was 220 L/person/day and 20 L/person for visitor. Thus, the TP loading of the entire watershed was 5,572 kg/year which consisted of 5,509 kg/year from domestic wastewater and 63 kg/year from leisure activities.

According to the Carlson trophic state index for water quality of the reservoir, the water quality condition in the Feitsui Reservoir is in the range of mesotrophic and eutrophic (Kuo et al. 2003). The nutrient loads from nonpoint agricultural and tourist activities are mainly pollutant sources. The historical water quality data including water temperature, pH, electrical conductivity, chemical oxygen demand, turbidity, suspended solids, total hardness, dissolved oxygen, chlorophyll *a*, total phosphorus, ammonia nitrogen, and nitrate nitrogen from 1993 to 2011 were collected from the Feitsui Reservoir Administration Bureau and were analyzed. The statistical summary of water quality variables is shown in Table 1. For the dissolved oxygen, the minimum, mean, and maximum values are 3.37, 7.14, and 9.40 mg/L, respectively, in the reservoir.

Table 1 The statistical summary of the water quality variables in the Feitsui Reservoir

Variables	Min	Max	Mean	St. dev.	C.V.
Water temperature (°C)	15.70	32.50	24.07	4.21	0.18
pH	6.08	8.92	7.56	0.69	0.09
Electrical conductivity (μmho/cm, 25 °C)	55.90	144.00	80.62	12.44	0.15
COD (mg/L)	0.50	35.63	5.59	4.07	0.73
Turbidity (NTU)	0.02	102.00	3.15	7.62	2.42
Suspended solids (mg/L)	0.30	13.80	2.66	1.98	0.74
Total hardness (mg/L)	10.80	81.60	23.70	7.04	0.30
Total alkalinity (mg/L)	7.50	35.48	18.85	5.28	0.28
Dissolved oxygen (mg/L)	3.37	9.40	7.14	1.11	0.16
Chlorophyll *a* (μg/L)	0.10	11.40	2.65	2.04	0.77
Total phosphorus (μg/L)	3.00	162.00	20.99	18.21	0.87
Ammonia nitrogen (mg/L)	0.01	0.69	0.11	0.11	0.99
Nitrate nitrogen (mg/L)	0.01	1.32	0.47	0.17	0.36

St. Dev. standard deviation,
C.V. coefficient of variation
(St. Dev./Mean)

Back propagation neural network (BPNN)

A back propagation neural network (BPNN) was applied to predict the dissolved oxygen in the Feitsui Reservoir. The BPNN, which was proposed by Rumelhart et al. (1986), is the most prevalent model in supervised learning models of ANN. The model is a multiple-layer network with nonlinear differentiable transfer functions, and it can be used to solve numerous nonlinear problems. Input vectors and corresponding target vectors are used to train BPNNs until the models can approximate a specified minimum error or a maximum number of epochs. BPNNs with weightings, biases, a sigmoid layer, and a linear output layer can approximate any function with a finite number of discontinuities.

Figure 2 shows the architecture of the BPNN. In the figure, Pi is the input vector; IW and b1 are weights and biases, respectively, between the input layer and the hidden layer; trans. is the transfer function; and LW and b2 are weight and biases, respectively, between the hidden layer and the output layer. As a result of their ability to extrapolate beyond the range of training data, the most commonly used transfer functions are sigmoid transfer functions in the hidden layer and linear transfer functions in the output layer. The connections between input and hidden layer neurons and between hidden and output layer neurons can be described by the following equations:

$$a1 = f(\mathrm{IW} \times \mathrm{Pi} + b1) \quad (1)$$

$$a2 = f(\mathrm{LW} \times \mathrm{Pi} + b2) \quad (2)$$

where a1 and a2 are the values of the hidden layer and the output layer, respectively. A hyperbolic tangent sigmoid transfer function, Eq. (3), and a linear transfer function, Eq. (4), are used in the hidden layer and the output layer.

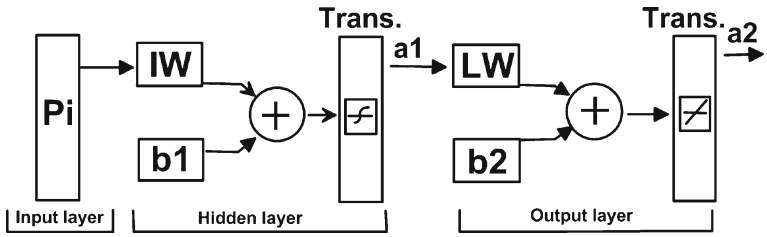

Fig. 2 Architecture of the back propagation neural network (BPNN)

$$f(x) = \frac{2}{(1 + e^{-2x}) - 1} \tag{3}$$

$$f(x) = x \tag{4}$$

Prior to the training and testing phases, it is often useful to scale the inputs and targets using the normalized equation in Eq. (5) so that the data always fall within a specified range.

$$Y_N = (y_{\max} - y_{\min}) \times \left(\frac{x_i}{x_{\max} - x_{\min}}\right) - y_{\min} \tag{5}$$

where Y_N is the value after normalization; $x_{\min}$ and $x_{\max}$ denote the minimum and maximum of the data, respectively; and $y_{\min}$ and $y_{\max}$ are taken as 1 and −1. The network performance function is quantified by the mean square error (MSE). The performance of the network can be measured according to the MSE in Eq. (6):

$$\text{MSE} = \frac{\sum_N (a_2 - y_i)_N^2}{N} \tag{6}$$

where y_i represents the observed value and N is the total number of data points. When the leaning performance (MSE) is less than a specific tolerance (10^{-3} for this model), the iteration terminates.

In the present study, BPNN updates weight and bias values according to the Fletcher–Powell conjugate gradient (Fletcher and Powell 1963) and is a back propagation supervised algorithm. The artificial neural network model was implemented in MATLAB, in which the Fletcher–Powell conjugate gradient technique is available in the Neural Network Toolbox.

Adaptive neuro-fuzzy inference system (ANFIS)

ANFIS is a multilayer feed-forward network in which each node performs a particular function on incoming signals. Both square and circle node symbols are used to represent different properties of adaptive learning. To obtain the desired input–output characteristics, adaptive learning parameters are updated based on gradient learning rules, and ANFIS learns the rules and membership functions from the data (Jang 1993). The primary drawback of the ANFIS predicting model is the time-intensive training and parameter determination.

Essentially, we assume that the fuzzy inference system under consideration has two inputs, x_1 and x_2, and only one output, y. It is assumed that the rule base contains two

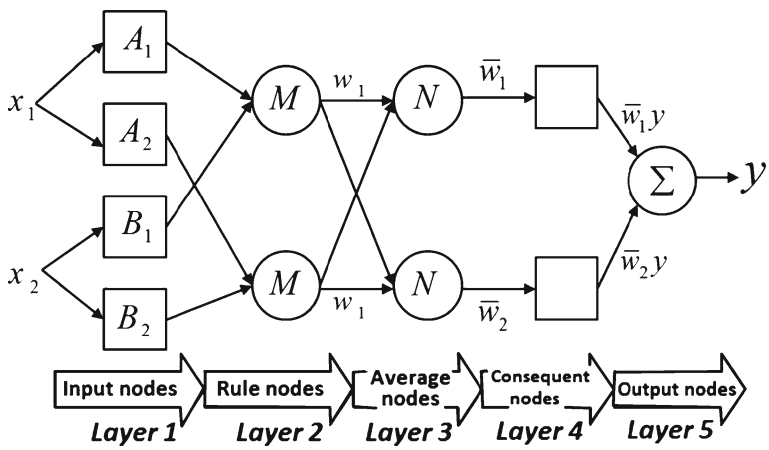

Fig. 3 Architecture of the adaptive network-based fuzzy interface system (ANFIS)

Table 2 Different input variables to predict dissolved oxygen in reservoirs

Literature	Input variables	Study site
Soyupak et al. (2003)	Season, different from major source, depth, and water temperature	Keban Dam Reservoir, Kuzgun Dam Reservoir, and Doğancı Dam Reservoir, Turkey
Sengorur et al. (2006)	NO_2-N, NO_3-N, water temperature, flow, and BOD	Turkey Reservoir
Chaves and Kojiri (2007)	Previous time of DO, BOD, TN, TP, chlorophyll *a*, and storage Present time of inflow, release, retention time, air temperature, and precipitation	Barra Bonita Reservoir, Brazil
Kuo et al. (2007)	Month, pH, chlorophyll *a*, NH_4-N, and NO_3-N	Te-Chi Reservoir, Taiwan
Ying et al. (2007)	Water temperature, turbidity, pH, alkalinity, chloride, NH_4-N, NO_2-N, and hardness	Yuqiao Reservoir, China
Rankovic et al. (2012)	pH, water temperature, NO_2-N, NH_4-N, Fe, Mn, and conductivity	Gruža Reservoir, Serbia

fuzzy IF–THEN rules of a first-order Sugeno fuzzy model (Takagi and Sugeno 1985):

Rule 1 If x_1 is A_1 and x_2 is B_1, then $y_1 = p_1x_1 + q_1x_2 + r_1$
Rule 2 If x_1 is A_1 and x_2 is B_1, then $y_2 = p_2x_1 + q_2x_2 + r_2$,

where A_i and B_i are the fuzzy sets and p_i, q_i, and r_i are the design parameters that will be determined during the training and testing processes. The architecture of ANFIS is shown in Fig. 3, in which circles represent fixed nodes and squares indicate adaptive nodes. A brief introduction of the ANFIS model follows.

Input nodes (layer 1): Each node i of this layer is a square node with a node function.

$$\begin{aligned} O_{1,i} &= \mu_{A_i}(x_1), i = 1,2 \\ O_{1,i} &= \mu_{B_{i-2}}(x_2), i = 3,4 \end{aligned} \tag{7}$$

where x_1 and x_2 are the inputs to node i, A_i and B_i are the linguistic labels, and μA_i and $\mu_{B_{i-2}}$ are the membership function for the A_i and B_i linguistic labels, respectively. The following bell-shaped membership function is used in this study:

$$\mu_{A_i} = \frac{1}{1 + \left|\frac{x_1 - c_i}{a_i}\right|^{2b_i}} \quad \mu_{B_{i-2}} = \frac{1}{1 + \left|\frac{x_2 - c_i}{a_i}\right|^{2b_i}} \tag{8}$$

where a_i, b_i, and c_i are the parameter sets. The parameters in this layer are the premise parameters.

Rule nodes (layer 2): Every node in this layer is a circle node labeled as M (Fig. 3). The outputs of this layer, which are called firing strengths ($O_{2,i}$), are the products of the corresponding degrees obtained from layer 1 (input layer).

$$O_{2,i} = w_i = \mu_{A_i}(x_1) \times \mu_{B_i}(x_1), i = 1,2 \tag{9}$$

Average nodes (layer 3): Every node in this layer is a circle node labeled as N (Fig. 3). The third layer contains fixed nodes that calculate the ratio of the firing strengths of the rules:

$$O_{3,i} = \overline{w}_i = \frac{w_i}{w_1 + w_2}, i = 1,2 \tag{10}$$

Table 3 The correlation coefficient (R) between dependent variable and dissolved oxygen

Variable	Correlation coefficient (R)
Water temperature (WT)	0.1691
pH	0.1571
Electrical conductivity (EC)	0.2108
COD	0.0916
Turbidity (TB)	0.1522
Suspended solids (SS)	0.1726
Total hardness (TH)	0.2844
Total alkalinity (TA)	0.2503
Chlorophyll *a*	0.0522
Total phosphorus	0.0888
Ammonia nitrogen (AN)	0.2381
Nitrate nitrogen	0.0214

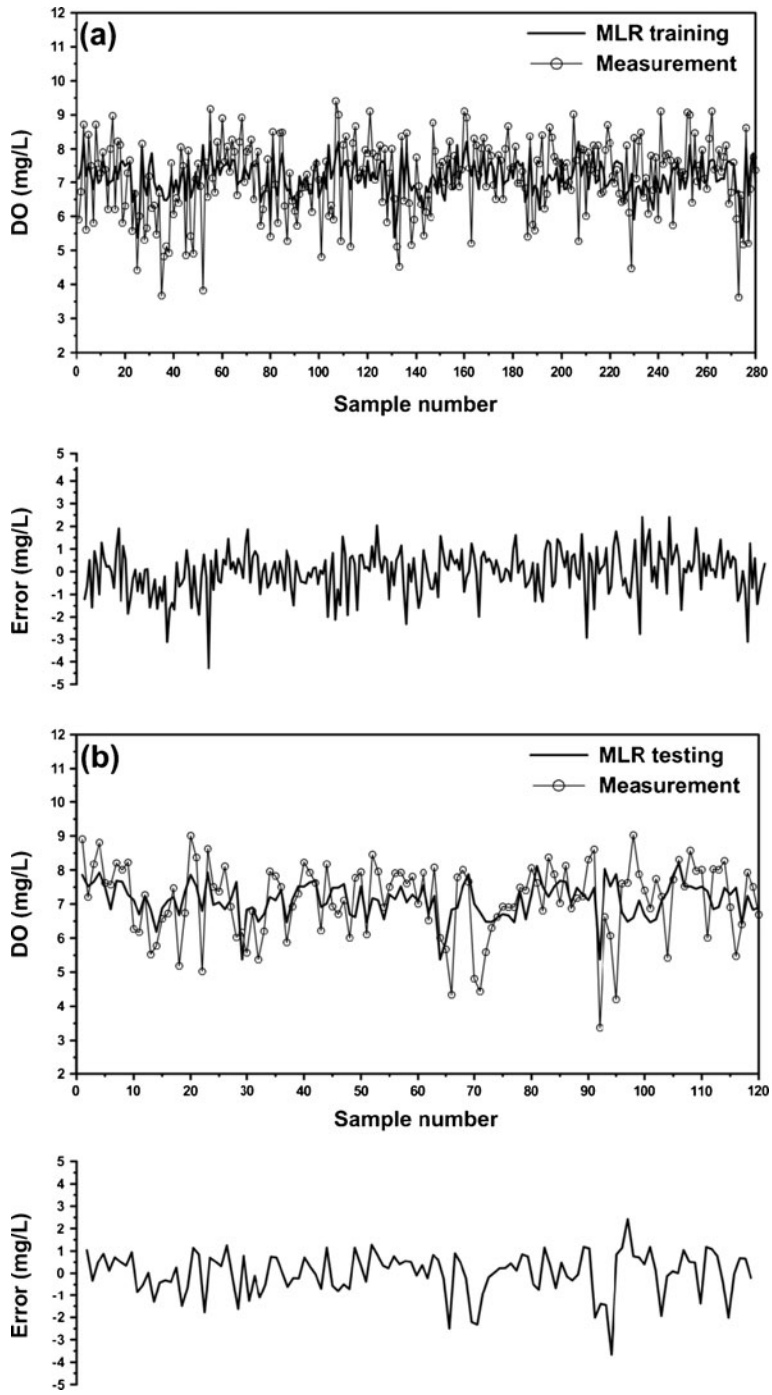

Fig. 4 Comparison of predicted and measured dissolved oxygen and the error with the MLR model for the **a** training phase and **b** testing phase

Consequent nodes (layer 4): The nodes in this layer are adaptive, and the output of each node is simply the product of the normalized firing strength and a first-order polynomial. Thus, the output and the function are defined by the following equation:

$$O_{4,i} = \overline{w}_i y_i = \overline{w}_i (p_i x + q_i y + r_i), i = 1, 2 \quad (11)$$

The parameters, p_i, q_i, and r_i in this layer are the coefficients of this linear combination and can be referred to as the consequent parameters.

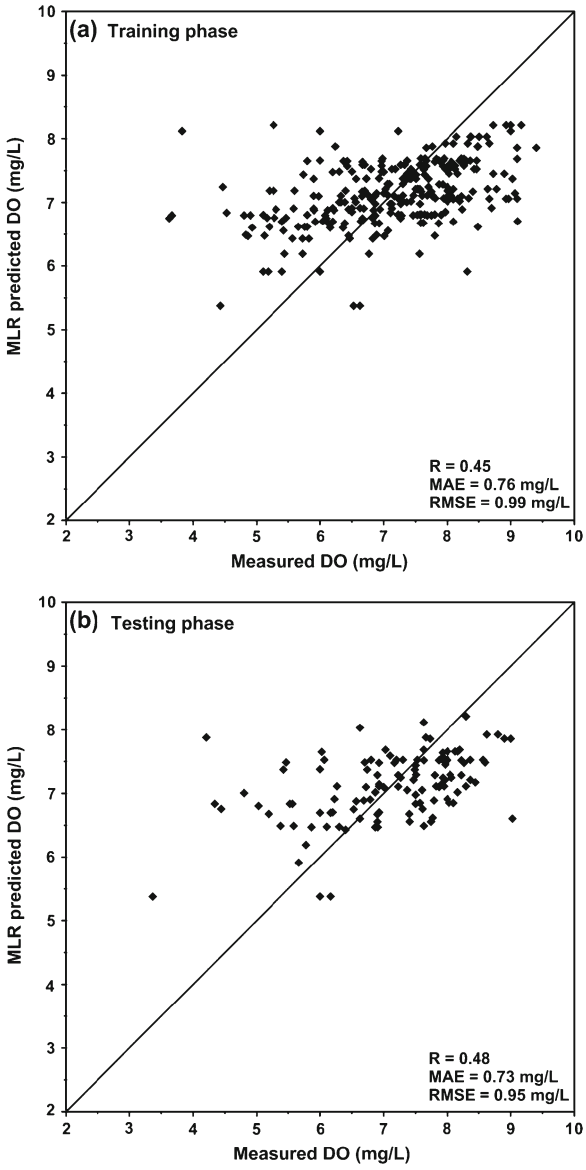

Fig. 5 Scatter plots of predicted and measured dissolved oxygen with the MLR model for the **a** training phase and **b** testing phase

Table 4 Performance evaluation for the multilinear regression model and artificial neural network models

Model	Training phase			Testing phase		
	MAE (mg/L)	RMSE (mg/L)	*R*	MAE (mg/L)	RMSE (mg/L)	*R*
MLR	0.76	0.99	0.45	0.73	0.95	0.48
BPNN	0.70	0.94	0.51	0.73	0.98	0.50
ANFIS	0.37	0.50	0.89	0.37	0.52	0.89

Output nodes (layer 5): The single node computes the overall output by summing all of the incoming signals.

$$O_{5,1} = \sum_{i=1}^{2} w_i y_i = \frac{\sum_{i=1}^{2} w_i y}{w_1 + w_2} \tag{12}$$

The details and mathematical background for these algorithms can be found in Jang (1993) and Nayak et al. (2004).

Indices of simulation performance

To determine the performance of the MLR and ANN models, three criteria were adopted to compare the model results and the observational data, which were the mean absolute error (MAE), the root mean square error (RMSE), and correlation coefficient (*R*). These criteria are defined by the following equations:

$$\mathrm{MAE} = \frac{1}{N}\sum_{N} \left|(C_\mathrm{p})_N - (C_\mathrm{m})_N\right| \tag{13}$$

$$\mathrm{RMSE} = \sqrt{\frac{1}{N}\sum_{N} \left[(C_\mathrm{p})_N - (C_\mathrm{m})_N\right]^2} \tag{14}$$

$$R = \frac{\sum_{N} \left[(C_\mathrm{p})_N - \overline{C_\mathrm{p}}\right]\left[(C_\mathrm{m})_N - \overline{C_\mathrm{m}}\right]}{\sqrt{\sum_{N} \left[(C_\mathrm{p})_N - \overline{C_\mathrm{p}}\right]^2 \sum_{N} \left[(C_\mathrm{m})_N - \overline{C_\mathrm{m}}\right]^2}} \tag{15}$$

where N is the total number of data points, C_p is the predicted dissolved oxygen, C_m is the measured dissolved oxygen, and $\overline{C_\mathrm{p}}$ and $\overline{C_\mathrm{m}}$ denote the average predicted and measured dissolved oxygen, respectively.

Results and discussion

Selecting the input variables

The selection of appropriate set of input variables for the MLR and ANN models is important for predicting the dissolved oxygen in reservoirs. Several researchers have used different water quality variables to serve as the model input and to predict the dissolved oxygen in

Table 5 Parameters used in the BPNN model

Model	Input nodes		Hidden nodes	Output nodes		Learning rate	Momentum	Iteration
	Number	Variable		Number	Variable			
BPNN	8	A	40	1	Dissolved oxygen	0.001	0.3	650

"A" represents the variables including water temperature, pH, conductivity, turbidity, suspended solids, total hardness, total alkalinity, and ammonium nitrogen

reservoirs. Table 2 presents the summary of different input variables used in their ANN models.

In order to find the relative importance and contribution of the input variables to the model output, the linear regression between different dependent variables and DO was conducted. Totally, 400 data sets collected from 1993 to 2011 were used for analyses. The available set of data was divided into two sections as training and test sets. For the training and testing phases using the MLR and ANN models, 70 % (i.e., 280 data sets) and 30 % (i.e., 120 data sets) of total data sets were used, respectively. Table 3 shows the correlation coefficient (R) between different dependent variables and DO concentration. It can be seen that the most effective inputs are determined as water temperature, pH, conductivity, turbidity, suspended solids, total hardness, total alkalinity, and ammonium nitrogen, because the correlation coefficient (R) is greater than 0.1 to be set as the threshold for selecting the water quality parameters. On the other hand, chemical oxygen demand (COD), chlorophyll *a*, total phosphorus, and nitrate nitrogen are found to be the least effective parameters.

DO prediction with the multilinear regression model

The simple multilinear regression model is used to predict the DO concentration. The multilinear regression in Eq. (16) was obtained from the input variables.

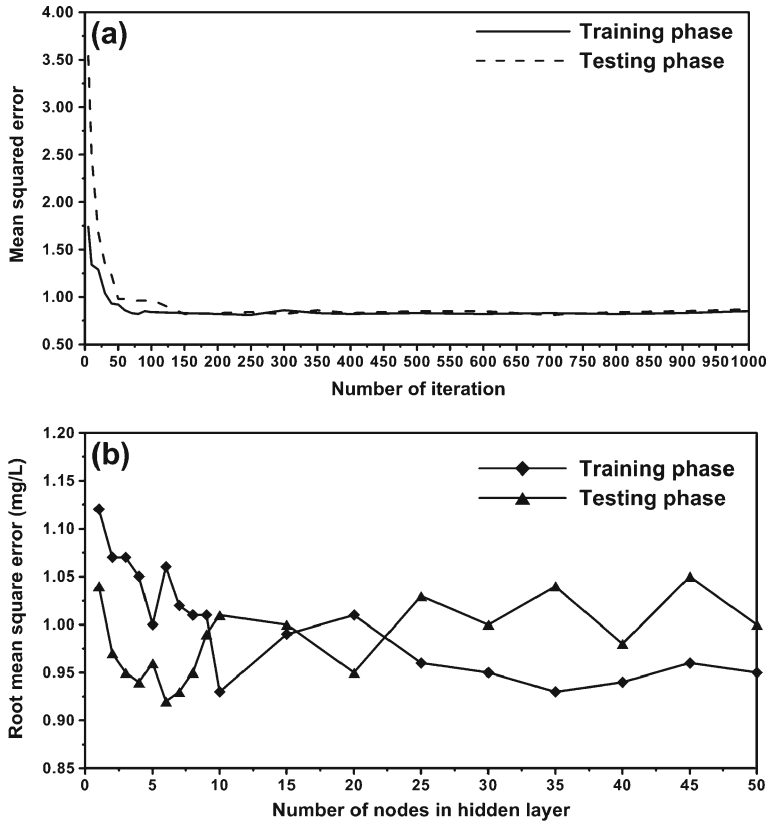

Fig. 6 **a** Variation of mean square error (MSE) with iterations and **b** effect of the node number in hidden layer on the root mean square error (RMSE)

$$DO = -0.1009 \times WT + 0.564 \times pH - 0.0057 \times EC - 0.0009 \times TB - 0.008 \times SS - 0.0378 \times TH - 0.0299 \times TA - 1.6138 \times AN + 7.318 \quad (16)$$

where WT is the water temperature, pH is the pH value, EC is the electrical conductivity, TB is the turbidity, SS is the suspended solids, TH is the total hardness, TA is the total alkalinity, and AN is the ammonia nitrogen.

Equation (16) was used to predict the DO concentration for the training and testing phases. Figure 4 presents the measured and model-predicted values of DO for the training and testing phases using the

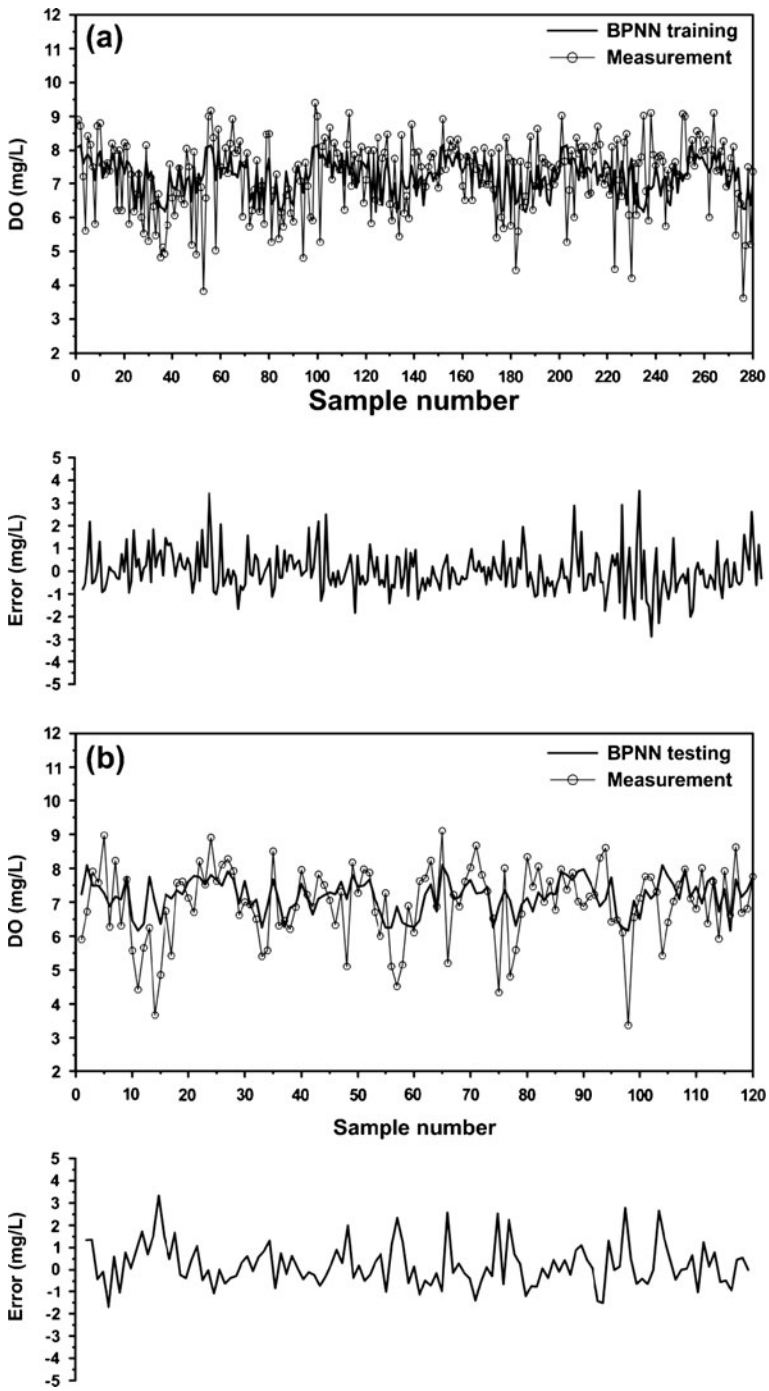

Fig. 7 Comparison of predicted and measured dissolved oxygen and the error with the BPNN model for the **a** training phase and **b** testing phase

multilinear regression model and Fig. 5 shows the scatter plots. The error values, representing the predicted DO minus measured DO, are also showed in Fig. 4. The performance evaluation is presented in Table 4. The MAE, RMSE, and *R* values for the training phase are 0.76 mg/L, 0.99 mg/L, and 0.45, while these values for testing are 0.73 mg/L, 0.95 mg/L, and 0.48, respectively. Akkoyunlu et al. (2011) applied two ANN models and MLR model to estimate the DO concentration in Lake Iznik, Turkey and found that the MLR model has less accuracy to predict the DO. Their conclusions are similar with our study in which the MLR model for predicting DO provides low accuracy.

DO prediction with the BPNN model

The BPNN model was constructed and tested to determine the optimum number of nodes in the hidden layer and the transfer functions. The selection of an appropriate number of nodes in the hidden layer is very important because an excessive large number of nodes may result in overfitting, while an insufficient number of nodes may not capture the information adequately.

For a given input set, the BPNN model produced an output, and this response was compared to the known desired response of each neuron. The weights of the neural network were then iteratively changed to correct or reduce the error between the neuron output and the desired response. The weights were continually changed until the total error of the entire training set was reduced below the accepted error level.

The architecture of the best BPNN model for DO in the reservoir is illustrated in Table 5. The best network architecture (i.e., the number of hidden nodes, the number of iterations, the learning rate, and the momentum coefficient) was obtained by trial and error, based on the MSE and RMSE values from the training and testing phases.

Figure 6a shows the MSE for the training and testing phases as a function of the number of iterations. After the number of iterations exceeded 650, the MSE did not change significantly. Therefore, 650 iterations were used for BPNN training and testing. In this study, a learning rate of 0.001 and a momentum coefficient of 0.3 were used. Figure 6b shows the effect of changing the number of hidden nodes on the RMSE of the data set during the training and validation. To yield the optimal number of nodes in the hidden layer, 40 hidden nodes in the BPNN were selected during the training and testing phases.

Figure 7 presents the measured and model-predicted values of DO for the training and testing phases. Figure 8 shows the scatter plots of measured and predicted DO for the training and testing phases. The MAE, RMSE, and *R* values for the training phase are 0.70 mg/L, 0.94 mg/L, and 0.51, while these values for the testing phase are 0.73 mg/L, 0.98 mg/L, and 0.50, respectively. Kuo et al. (2007) applied the BPNN model to predict the DO in the

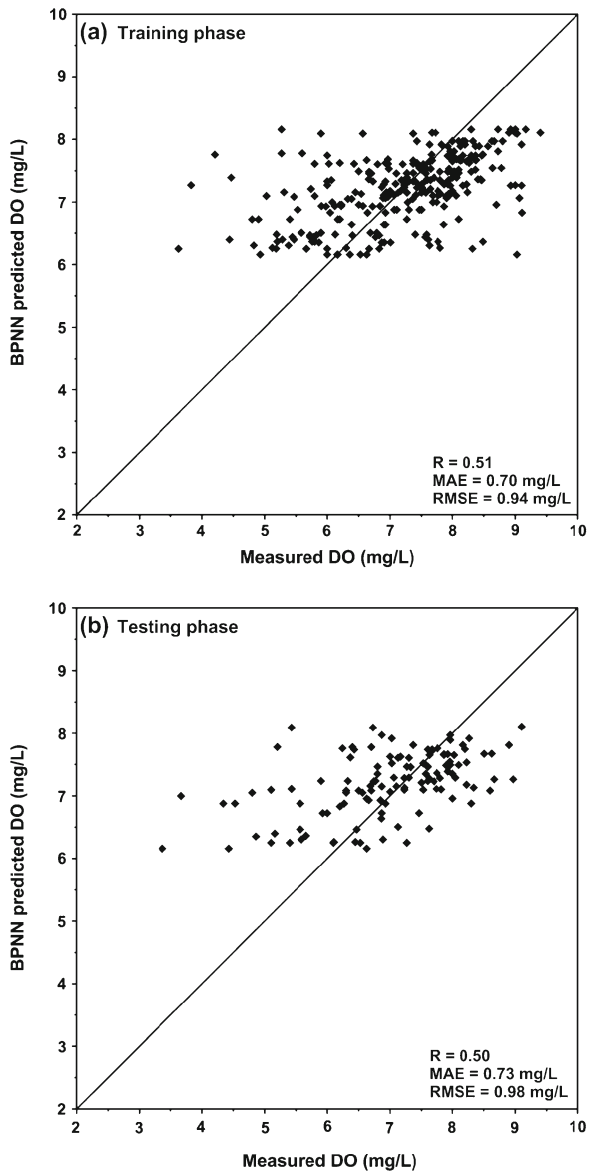

Fig. 8 Scatter plots of predicted and measured dissolved oxygen with the BPNN model for the **a** training phase and **b** testing phase

Te-Chi Reservoir. The correlation coefficients (R) for predicted and measured DO are 0.75 and 0.72, respectively, for the training and testing phases. Ying et al. (2007) used the BPNN approach to predict the DO concentration in the Yuqiao Reservoir, China. The correlation coefficient of 0.94 was calculated between the measured and simulated DO values. In the present study, the correlation coefficient (R) for DO training and testing

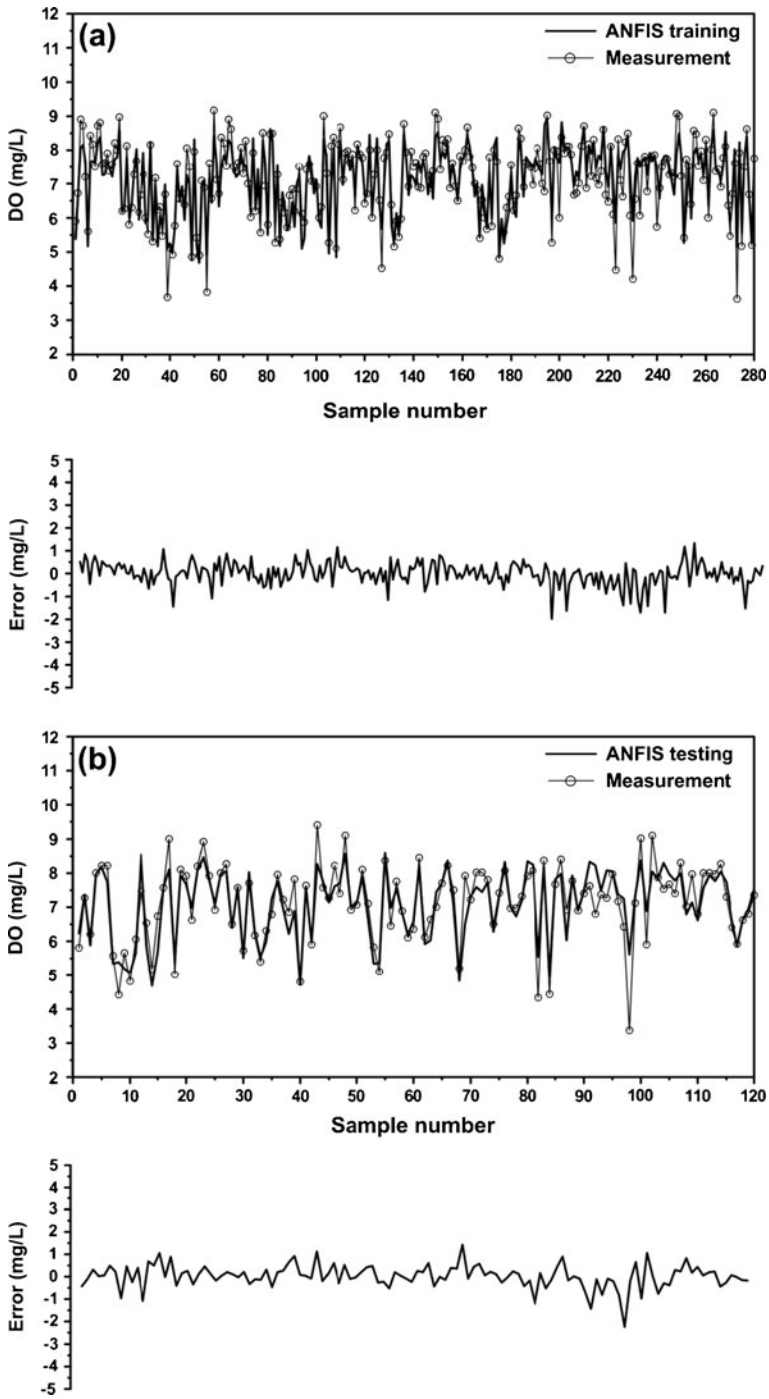

Fig. 9 Comparison of predicted and measured dissolved oxygen and the error with the ANFIS model for the **a** training phase and **b** testing phase

with the BPNN model is higher than that with the multilinear regression model. However, the correlation coefficient (R) obtained in the Feitsui Reservoir with the BPNN model is lower than that reported by other studies in reservoirs.

DO prediction with the ANFIS model

Due to the poor performance of the multilinear regression model and BPNN model, the alternative approach, ANFIS model, was used to predict the DO concentration. In the ANFIS structure, each variable may have several values (in terms of rules), and each rule includes several parameters of membership functions. In this study, subtractive fuzzy clustering is used to establish the rule-based relationship between the input and output variables. Subtractive clustering is a technique for automatically generating fuzzy inference systems by detecting clusters in input–output training data. The number of membership functions for each input of ANFIS was set to 3. Membership function types for inputs and output were selected as Gaussian (or bell-shaped) and linear, respectively.

Figures 9 and 10 show the comparison of model-predicted DO and measured DO for the training and testing phases and scatter plots, respectively. The MAE, RMSE, and R values for the training phase are 0.37 mg/L, 0.50 mg/L, and 0.89, while these values for the testing phase are 0.37 mg/L, 0.52 mg/L, and 0.89, respectively. The performances with the ANFIS model are better than those with the multilinear regression and BPNN models.

Rankovic et al. (2012) applied the ANFIS approach to predict the DO concentration in the Gruža Reservoir, Serbia and concluded that the coefficients of correlation for training and testing data sets were 0.8217 and 0.8856, respectively. Their results have lower performance compared to our study in the Feitsui Reservoir.

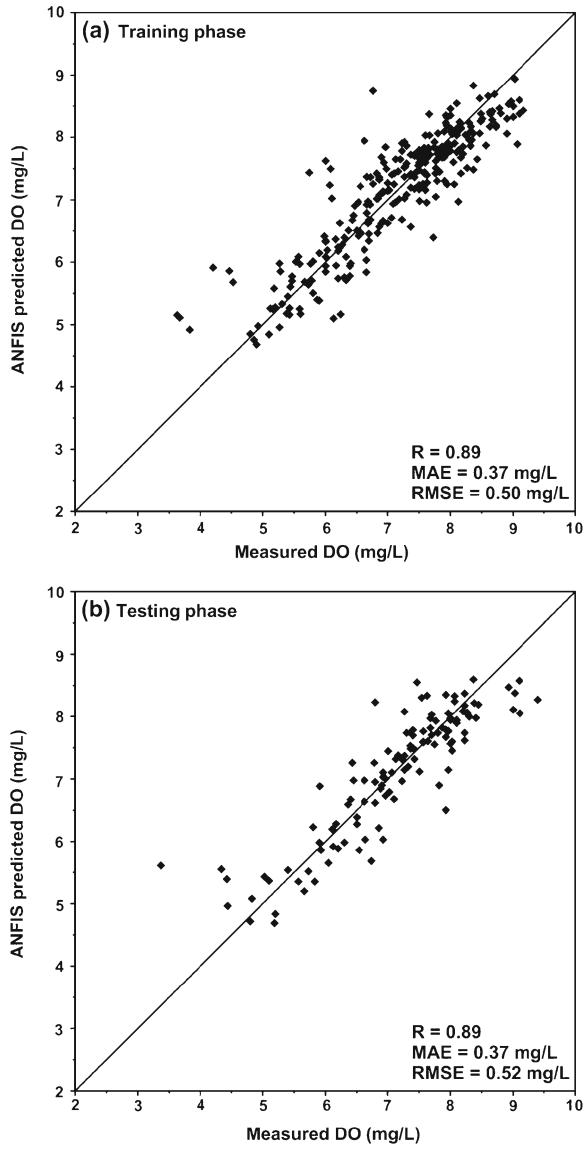

Fig. 10 Scatter plots of predicted and measured dissolved oxygen with the ANFIS model for the **a** training phase and **b** testing phase

Conclusions

Two ANN models (BPNN and ANFIS approaches) and MLR model were developed to predict the DO of reservoir. The performances of the ANN models and MLR model were tested using mean absolute error, root mean square error, and correlation coefficient. The linear regression between DO and dependent variable was used to select the major input water quality variables for the ANN models and MLR model.

The models were then constructed to predict the DO in the Feitsui Reservoir. The results show that the correlation coefficients between predicted and measured DO values are 0.45 and 0.48, respectively, for the training and testing phases with the multilinear regression model, 0.51 and 0.50 with the BPNN model, and 0.89 and 0.89 with the ANFIS model. The ANN models can preserve nonlinear characteristics between input and output variables, which are superior to the traditional statistical model (i.e., MLR model). The predictive results show that the ANFIS model

is superior to the BPNN and multilinear regression models. The application of the suitable neural network to predict dissolved oxygen gives satisfactory results. The proposal model can be a very efficient tool and useful alternative for the computation of other water quality variables, such as chlorophyll *a*, total phosphorus, and suspended solids in reservoirs.

Acknowledgments The project under which this study was conducted is supported by the National Science Council, Taiwan, under grant no. NSC 100-2625-M-239-001. The authors would like to express their appreciation to the Feitsui Reservoir Administration Bureau for providing the observational data.

References

Akkoyunlu, A., Altun, H., & Cigizoglu, H. K. (2011). Depth-integrated estimation of dissolved oxygen in a lake. *Journal of Environmental Engineering, 137*(10), 961–967.

Boano, F., Revelli, R., & Ridolfi, L. (2006). Stochastic modelling of DO and BOD components in a stream with random inputs. *Advances in Water Resources, 29*(9), 1341–1350.

Bonnet, M. P., & Poulin, M. (2004). DyLEM-1D: a 1D physical and biochemical for plankton succession, nutrients and dissolved oxygen cycling application to hyper-eutrophic reservoir. *Ecological Modelling, 180*(2–3), 317–344.

Chaves, P., & Kojiri, T. (2007). Conceptual fuzzy neural network model for water quality simulation. *Hydrological Processes, 21*(5), 634–646.

Chen, Y. J., & Wu, S. C. (2006). Behavior of storm-induced suspension interflow in subtropical Feitsui Reservoir, Taiwan. *Limnology and Oceanography, 51*(2), 1125–1133.

Cho, K. H., Park, Y., Kang, J. H., Ki, S. J., Cha, S., Lee, S. W., & Kim, J. H. (2009). Interpretation of seasonal water quality variation in the Yeongsan Reservoir, Korea using multivariate statistical analysis. *Water Science and Technology, 59*(11), 2219–2226.

Chou, W. S., Lee, T. C., Lin, J. Y., & Yu, S. L. (2007). Phosphorus load reduction goals for Feitsui Reservoir watershed, Taiwan. *Environmental Monitoring and Assessment, 131*(1–3), 385–408.

Curi, W. F., Unny, T. E., & Kay, J. J. (1995). A stochastic physical system approach to modeling river water quality. *Stochastic Hydrology and Hydraulics, 9*(2), 117–132.

Fletcher, R., & Powell, M. J. D. (1963). A rapid convergent descent method for minimization. *The Computer Journal, 6*(2), 163–168.

Gardner, M. W., & Dorling, S. R. (1998). Artificial neural network (the multilayer perceptron)—a review of application in atmospheric sciences. *Atmospheric Environment, 32*(14–15), 2626–2636.

Jang, J. S. R. (1992). Self-learning fuzzy controllers based on temporal back propagation. *IEEE Transactions on Neural Networks, 3*(5), 714–723.

Jang, J. S. R. (1993). ANFIS: adaptive-network-based fuzzy inference system. *IEEE Transactions on Systems, Man, Cybernetics, 23*(3), 665–685.

Karakaya, N., Evrendilek, F., & Gungor, K. (2011). Modeling and validating long-term dynamics of diel dissolved oxygen with particular reference to pH in a temperate shallow lake (Turkey). *Clean-Soil, Air, Water, 39*(11), 966–971.

Keskin, M. E., Taylan, D., & Terzi, O. (2006). Adaptive neural-based fuzzy inference system (ANFIS) approach for modelling hydrological time series. *Hydrological Sciences Journal, 51*(4), 588–598.

Kuo, J. T., Liu, W. C., Lin, R. T., Lung, W. S., Yang, M. D., Yang, C. P., & Chu, S. C. (2003). Water quality modeling for the Feitsui Reservoir in northern Taiwan. *Journal of the American Water Resources Association, 39*(4), 671–687.

Kuo, J. T., Hsieh, M. H., Lung, W. S., & She, N. (2007). Using artificial network for reservoir eutrophication prediction. *Ecological Modelling, 200*(1–2), 171–177.

Lindim, C., Pinho, J. L., & Vieira, J. M. P. (2011). Analysis of spatial and temporal patterns in a large reservoir using water quality and hydrodynamic modeling. *Ecological Modelling, 222*(14), 2485–2494.

Liu, W. C., Chen, W. B., & Nobuaki, K. (2009). Impact of phosphorus load reduction on water quality in a stratified reservoir-eutrophication modeling study. *Environmental Monitoring and Assessment, 159*(1–4), 393–406.

Najah, A., El-Shafie, A., Karim, O. A., Jaafar, O., & El-Shafie, A. H. (2011). An application of different artificial intelligences techniques for water quality prediction. *International Journal of Physical Sciences, 6*(22), 5298–5308.

Najah, A., El-Shafie, A., Karim, O. A., & Jaafar, O. (2012). Water quality prediction model utilizing integrated wavelet-ANFIS model with cross-validation. *Neural Computing and Applications, 21*(5), 833–841.

Nayak, P. C., Sudheer, K. P., Ragan, D. M., & Ramasastri, K. S. (2004). A neuro fuzzy computing technique for modeling hydrological time series. *Journal of Hydrology, 291*(1–20), 52–66.

Nourani, V., & Komasi, M. (2013). A geomorphology-based ANFIS model for multi-station modeling of rainfall-runoff process. *Journal of Hydrology, 490*, 41–55.

Palani, S., Liong, S. Y., & Tkalich, P. (2008). An ANN application for water quality forecasting. *Marine Pollution Bulletin, 56*(9), 1586–1597.

Rankovic, V., Radulovic, J., Radojevic, I., Ostojic, A., & Comic, L. (2012). Prediction of dissolved oxygen in reservoirs using adaptive network-based fuzzy inference system. *Journal of Hydroinformatics, 14*(1), 167–179.

Rezaeianzadeh, M., Tabari, H., & Yazdi, A. A. (2013). Flood flow forecasting using ANN, ANFIS and regression models. *Neural Computing and Applications*. doi:10.1007/s00521-013-1443-6.

Rucinski, D. K., Beletsky, D., DePinto, J. V., Schwab, D. J., & Scavia, D. (2010). A simple 1-dimensional, climate based dissolved model to central basin of Lake Erie. *Journal of Great Lakes Research, 36*(3), 465–476.

Rumelhart, D. E., Hinton, G. E., & Williams, R. J. (1986). Learning representations by back-propagating errors. *Nature, 323*, 533–536.

Sengorur, B., Dogan, E., Koklu, R., & Samamdar, A. (2006). Dissolved oxygen estimation using artificial neural network for water quality control. *Fresenius Environmental Bulletin, 15*(9), 1064–1067.

Singh, K. P., Basant, A., Malik, A., & Jain, G. (2009). Artificial neural network modeling of the river water quality—a case study. *Ecological Modelling, 220*(6), 888–895.

Soltani, F., Kerachian, R., & Shirangi, E. (2010). Developing operating rules for reservoirs considering the water quality issues: application of ANFIS-based surrogate models. *Expert Systems with Applications, 37*(9), 6639–6645.

Soyupak, S., Karaer, F., Gurbuz, H., Kivrak, E., Senturk, E., & Yazici, A. (2003). A neural network-based approach for calculating dissolved oxygen profiles in reservoirs. *Neural Computing & Applications, 12*(3–4), 166–172.

Stansbury, J., Kozimor, L., Admiraal, D., & Dove, E. (2008). Water quality modeling of the effects of macrophytes on dissolved oxygen in a shallow tailwater reservoir. *Lake and Reservoir Management, 24*(4), 339–348.

Takagi, T., & Sugeno, M. (1985). Fuzzy identification of systems and its applications to modeling and control. *IEEE Transactions on Systems, Man, Cybernetics, 15*(1), 116–132.

Talei, A., Chua, L. H. C., & Wong, T. S. W. (2010). Evaluation of rainfall and discharge inputs used by adaptive network-based fuzzy inference system (ANFIS) in rainfall-runoff modeling. *Journal of Hydrology, 319*(3–4), 248–262.

TWMC (Taipei Water Management Committee). (2003). *A report of implementation efficiency on protecting water quality/quantity for Taipei Water Source Domain*. Taipei: MOEA (in Chinese).

Wen, X., Fang, J., Diao, M., & Zhang, C. (2013). Artificial neural network modeling of dissolved oxygen in the Heihe River, Northwestern China. *Environmental Monitoring and Assessment, 185*(5), 4361–4371.

White, J. D., Prochnow, S. J., Filstrup, C. T., Scott, J. T., Byars, B. W., & Zygo-Flynn, L. (2010). A combined watershed-water quality modeling analysis of the Lake Waco reservoir: I. Calibration and confirmation of predicted water quality. *Lake and Reservoir Management, 26*(2), 147–158.

Yao, J. Y., Xiao, P., Zhang, Y. H., Zhan, M., & Cheng, J. W. (2011). A mathematical model of algal blooms based on the characteristics of complex networks theory. *Ecological Modelling, 222*(20–22), 3727–3733.

Ying, Z., Jun, N., Fuvi, C., & Liang, G. (2007). Water quality forecast through application of BP neural network at Yuqiao reservoir. *Journal Zhejiang University-Science A, 8*(9), 1482–1487.